Biosensors and Bioelectronics 85 (2016) 930–934

Contents lists available at ScienceDirect

Biosensors and Bioelectronics

journal homepage: www.elsevier.com/locate/bios

Ag nanoclusters could efficiently quench the photoresponse of CdS quantum dots for novel energy transfer-based photoelectrochemical bioanalysis

Ling Zhang [a,b], Yue Sun [b], Yan-Yu Liang [a,*], Jian-Ping He [a], Wei-Wei Zhao [b,*], Jing-Juan Xu [b], Hong-Yuan Chen [b]

[a] School of Materials Science and Technology, Nanjing University of Aeronautics and Astronautics, Nanjing 211106, China
[b] State Key Laboratory of Analytical Chemistry for Life Science and Collaborative Innovation Center of Chemistry for Life Science, School of Chemistry and Chemical Engineering, Nanjing University, Nanjing 210023, China

ARTICLE INFO

Article history:
Received 16 April 2016
Received in revised form
26 May 2016
Accepted 7 June 2016
Available online 8 June 2016

Keywords:
Photoelectrochemical
Bioanalysis
Quantum dots
Nanoclusters
Energy transfer

ABSTRACT

Herein the influence of ultrasmall Ag nanoclusters (Ag NCs) against CdS quantum dots (QDs) in a photoelectrochemical (PEC) nanosystem was exploited for the first time, based on which a novel PEC bioanalysis was successfully developed via the efficient quenching effect of Ag NCs against the CdS QDs. In a model system, DNA assay was achieved by using molecular beacon (MB) probes anchored on a CdS QDs modified electrode, and the MB probes contain two segments that can hybridize with both target DNA sequence and the label of DNA encapsulated Ag NCs. After the MB probe was unfolded by the target DNA sequence, the labels of oligonucleotide encapsulated Ag NCs would be brought in close proximity to the CdS QDs electrode surface, and efficient photocurrent quenching of QDs could be resulted from an energy transfer process that originated from NCs. Thus, by monitoring the attenuation in the photocurrent signal, an elegant and sensitive PEC DNA bioanalysis could be accomplished. The developed biosensor displayed a linear range from 1.0 pM to 10 nM and the detection limit was experimentally found to be of 0.3 pM. This work presents a feasible signaling principle that could act as a common basis for general PEC bioanalysis development.

1. Introduction

Photoelectrochemical (PEC) bioanalysis has recently gained substantial momentum for its potential in future bioanalysis (Zhao et al., 2014; Gill et al., 2008; Shu et al., 2016; Yan et al., 2015; Zhang et al., 2013c; Li et al., 2016; Tang et al., 2015). Analysts in this field are now infatuated with exploiting exquisite signaling mechanisms for innovative applications (Zhang et al., 2012b; Zhuang et al., 2015; Wang et al., 2015; Long et al., 2011; Wang et al., 2014a, Sun et al., 2015). Among various efforts, exciton-plasmon interactions (EPI) between the noble metal nanoparticles (NPs) and quantum dots (QDs) have been demonstrated as a unique route for ingenious PEC biosensing purposes (Zhao et al., 2011, Zhao et al., 2012). Such interesting mechanism was then used for tentative bioanalysis with a simple DNA hybridization model, which provided a feasible basis for elegant PEC bioassays and many recent protocols were proposed for addressing different targets (Zeng et al., 2013; Ma et al., 2016). Despite the progress manifested in these works, the study in this field is still in its inception phase. Innovative bioanalytical formats with new signaling strategies are yet highly needed for the further advancement of PEC bioanalysis.

As a versatile nanomaterial, noble metal nanoclusters (NCs) can exhibit molecule-like electronic transitions between highest occupied molecular orbital (HOMO) and lowest unoccupied molecular orbital (LUMO) energy levels due to the quantum confinement originated from their small sizes (Díez et al., 2011; Han et al., 2012; Link et al., 2002). Because of their unique electronic structures as well as physicochemical properties, NCs have attracted much attention recently and been widely used in biolabeling (Guével et al., 2012), biosensing (Gong et al., 2015; Liu et al., 2015; Zheng et al., 2015), and bioimaging (Wang et al., 2014b). For example, with its desirable photophysical characteristics, NCs are widely used for fluorescent (Zhang et al., 2012a, 2013a, 2013b; Yeh et al., 2010; Xiao et al., 2013) and electrochemiluminescent (ECL) bioanalysis (Li et al., 2011; Fang et al., 2011). Unfortunately, to date, there is no investigation on their behaviour upon QDs in a

* Corresponding authors.
E-mail addresses: liangyy403@126.com (Y.-Y. Liang), zww@nju.edu.cn (W.-W. Zhao).

http://dx.doi.org/10.1016/j.bios.2016.06.018
0956-5663/

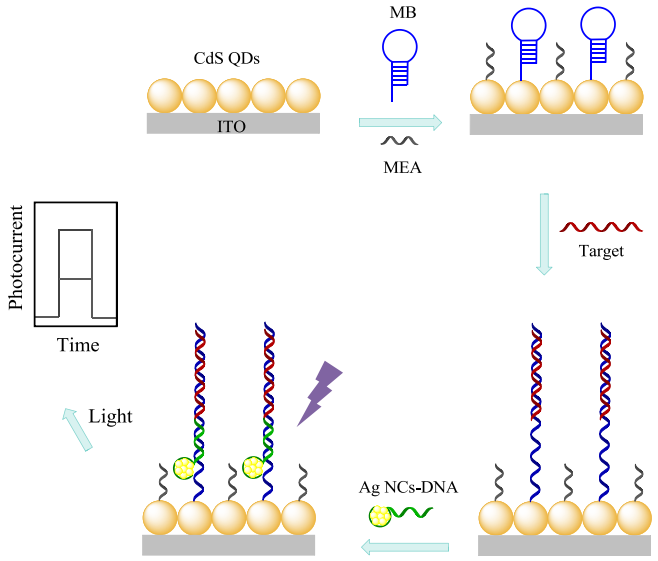

Scheme 1. Schematic illustration for the PEC DNA bioanalysis using the MB probe and Ag NCs.

judiciously designed PEC bioanalytical nanosystem.

Herein, we present the first exploitation on the influence of NCs against QDs in a PEC nanosystem, which demonstrated that efficient photocurrent quenching of QDs could be resulted from an energy transfer process that originated from NCs, and the unique phenomenon was then utilized for the DNA analysis in a model system. The analysis, by use of the oligonucleotide encapsulated Ag NCs and the CdS QDs, is depicted schematically in Scheme 1. As shown, CdS QDs were immobilized onto the indium tin oxide (ITO) electrode through the electrostatic interactions between the sequentially adsorbed positively charged poly(diallyldimethylammonium chloride) (PDDA) and thioglycolic acid (TGA) capped CdS QDs with an opposite charge. Thereafter, the molecular beacon (MB) probe, containing two segments that hybridize with target DNA sequence and the label of DNA encapsulated Ag NCs (Ag NCs-DNA), respectively, was anchored to the electrode via the classic carbodiimide-assisted amidation reaction and subsequently blocked with monoethanolamine (MEA). After the unfolding of the MB by the target DNA sequence, the labels of oligonucleotide encapsulated Ag NCs were hybridized with the rest part of the MB molecules, rendering the Ag NCs in close proximity to the CdS QDs. Upon proper conditions, the interparticles interaction between the Ag NCs and the CdS QDs could cause the attenuation in the photocurrent signal, based on which a novel strategy for PEC DNA biaoanalysis could be accomplished.

2. Experimental section

2.1. Materials and apparatus

The ITO slices (type N-STN-S1-10) were obtained from China Southern Glass Holding Co., Ltd.. $CdCl_2 \cdot 2.5H_2O$ was obtained from Shanghai Jinshan Tingxin Chemical. $Na_2S \cdot 9H_2O$ was obtained from Shanghai Lingfeng Chemical Reagent Co., LTD (Shanghai, China). PDDA (20%, w/w in water, molecular weight (200,000–350000)) were obtained from Sigma-Aldrich. 1-Ethyl-3-(3-dimethylaminopropyl) carbodiimide (EDC) was purchased from Fluka. *N*-Hydroxysuccinimide (NHS), ascorbic acid (AA), thioglycolic acid (TGA) and monoethanolamine (MEA) were purchased from Sinopharm Chemical Reagent Co., LTD (Shanghai, China). $AgNO_3$ was purchased from Aladdin. $NaBH_4$ was purchased from Tianjin Chemical Reagent Institute. All the synthetic oligonucleotides were purchased from GenScript Biotechnology Co., Ltd. (Nanjing, China) and the corresponding sequences were listed in Table S1 of Supplementary material. Washing buffer solution was 0.01 M PBS (pH 7.4). All other reagents were analytical grade and were used as received. All aqueous solutions including phosphate buffer solution (PBS) were prepared using ultra-pure water (Milli-Q, Millipore).

Transmission electron microscopy (TEM) was performed with a JEOL model 2000 instrument operating at 200 kV accelerating voltage. The UV–vis absorption spectra were obtained on a Shimadzu UV-3600 UV–vis–NIR photospectrometer (Shimadzu Co.). The X-ray photoelectron spectrum (XPS) was recorded on an ESCALAB 250 spectrometer (Thermo-VG Scientic Co. USA) with an ultrahigh vacuum generator. The fluorescence measurements were performed with a RF-5301 PC fluorometry (Shimadzu, Japan). PEC measurements were performed with a homemade PEC system: a 5 W LED lamp with monochromatic emitting at 410 nm was used as irradiation source to produce the monochromatic illuminating light on the front of the electrode. Photocurrent was measured on a CHI 750a electrochemical workstation (China) with a three-electrode system: a modified ITO electrode with a geometrical circular area (diameter-0.5 cm) as the working electrode, a Pt wire as the counter electrode, and a saturated Ag/AgCl electrode as the reference electrode. All the photocurrent measurements were performed at a constant potential of 0.0 V (versus Ag/AgCl). A 0.1 M PBS containing 0.1 M AA was used as the blank solution for photocurrent measurements, which was degassed by highly pure nitrogen for 15 min before PEC experiments and then kept over a N_2 atmosphere for the entire experimental process.

2.2. DNA bioanalysis development

Synthesis of TGA stabilized CdS QDs and Ag NCs-DNA, as well as the CdS QDs modification on the ITO electrode were described in Supplementary material. Then, the obtained CdS QDs modified electrodes were immersed in a solution containing 10 mM EDC and 20 mM NHS for 60 min at room temperature. After rinsing with the washing buffer solution, 25 μL of MB probe was dropped onto the surface of the electrode and incubated at 4 °C overnight, then immersed in 1 mM MEA solution at the same pH for about 2 h to Block nonspecific binding sites. Next, the electrode was rinsed again with the washing buffer solution and was incubated in 25 μL of target DNA solution at 37 °C for 2 h. After removal of excess target DNA by rinsed with the washing buffer solution, 25 μL of AgNCs-DNA probe was introduced onto the surface of the electrode and incubated at 25 °C in darkness for 2 h. Finally, after being washed, the obtained Ag NCs-labelled probe was served as the working electrode for the following PEC analysis. In order to obtain the stable photocurrent generation and to inhibit the photodissolution reaction of CdS QDs, the experiments were performed under the optimized conditions of 0.0 V potential and 0.1 M AA that acts as electron donor (Wang et al., 2009; Ma et al., 2015).

3. Results and discussion

3.1. Characterization of Ag NCs-DNA

The properties of Ag NCs strongly depend on the particles size, stabilizer, surrounding medium, and aggregation state (Shang et al., 2011; Richards et al., 2008). In this work, Ag NCs were synthesized using single sequence DNA (ssDNA) chain containing eight cytosine bases as a template and $NaBH_4$ as the reducing agent for reduction of Ag cation. Ag ions possess a high affinity to

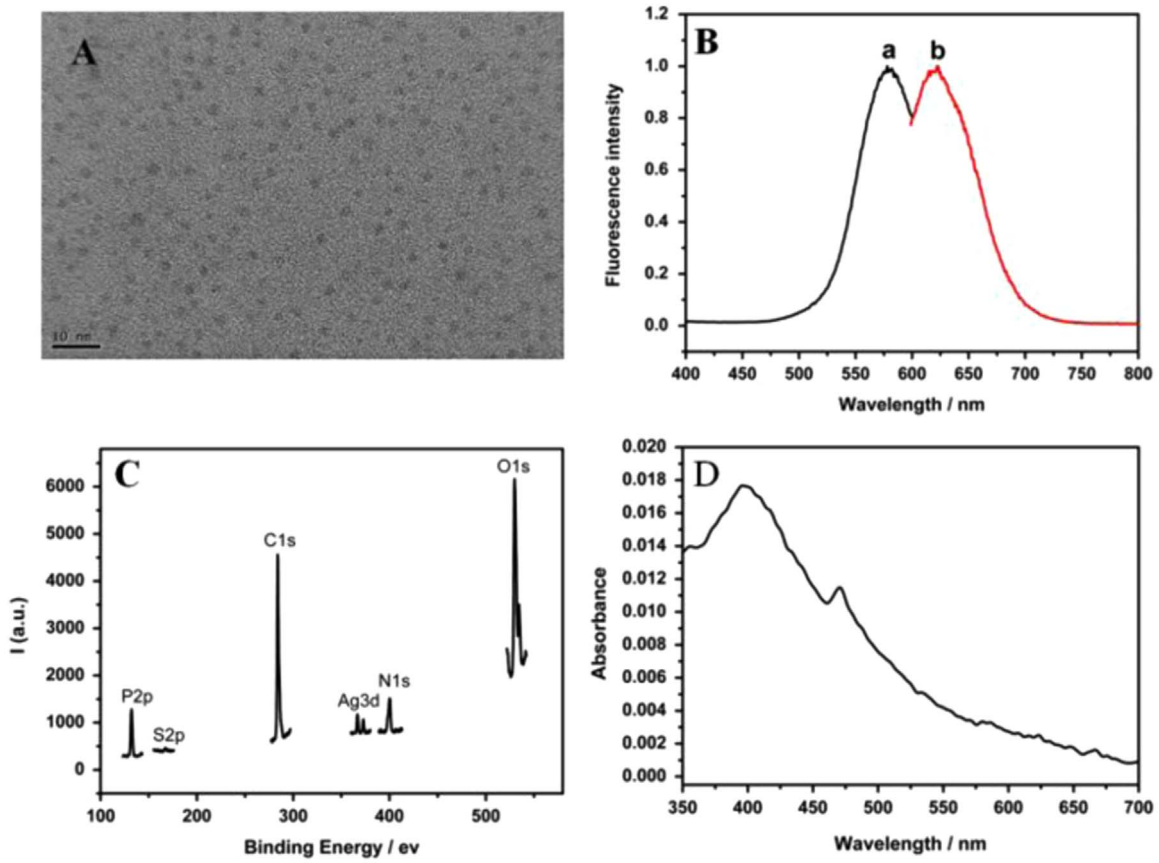

Fig. 1. (A) TEM image, (B) excitation (a) and emission (b), (C) XPS and (D) UV–vis spectra of the as-prepared Ag NCs-DNA.

cytosine bases on ssDNA (Ritchie et al., 2007), which provided templates and simultaneously acted as desirable stabilizers that advantageous for obtaining good size and size distribution of Ag NCs. The as-prepared Ag NCs were then characterized using various techniques. Fig. 1A shows the transmission electron microscopy (TEM) image of the Ag NCs, which clearly manifested that the Ag NCs were spherical with average diameter of ca. 2 nm, which could be attributed to the ssDNA stabilizer that stopped the Ag NCs from further growing once the desired size is reached. Such narrow size distribution is obviously useful for the subsequent bioanalytical application. Fig. 1B reveals the typical excitation and emission spectrum of the as-prepared Ag NCs, with maximal fluorescence excitation and emission at 577 and 619 nm, respectively. Fig. 1C displays the X-ray photoelectron spectroscopy (XPS) of the sample, the appearance of the Ag, P and S indicated the successful fabrication of Ag NCs-DNA. The detail of the XPS spectra was explained with Fig. S1. As further evidence, the UV–vis absorption spectrum of Ag NCs-DNA was performed as shown in Fig. S2. And Fig. 1D demonstrated the amplified spectrum of the Ag NCs, the peaks at 403 and 480 nm were consistent with the literature results (Dong et al., 2012), indicating the generation of ultrasmall Ag NCs.

3.2. Feasibility of the PEC DNA bioanalysis

The Ag NCs-DNA was then utilized for signal transduction in the proposed DNA bioanalysis. The biosensor development process was then monitored by the stepwise transient photocurrent responses upon the intermittent monochromatic light irradiation. As shown in Fig. 2, comparing with the initial intensity of CdS QDs electrode (curve a), the photocurrent decreased about 37% after anchoring MB and blocking by MEA (curve b), and such decrement

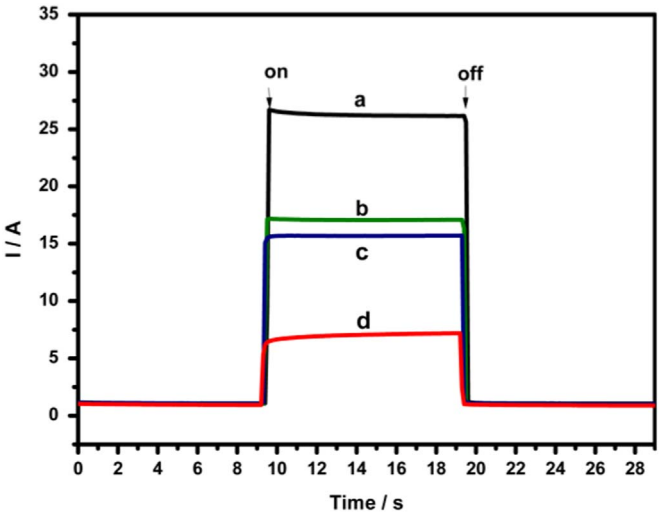

Fig. 2. Photocurrent intensity in 0.10 M PBS containing 0.10 M ascorbic acid of (a) CdS modified ITO electrode, (b) modified with 25 μL, 1 μM MB and blocked by MEA, (c) hybridized with target DNA, (d) linked with Ag NCs/ DNA. The concentration of target DNA was 1.0×10^{-6} M. The working potential was 0.0 V and the excitation wavelength was 410 nm.

should be attributed to that the anchoring layer impeded the diffusion of electron donor (AA) to the surface of CdS QDs. Further capture of target DNA on the electrode by the specific binding induced unfolding of the MB caused a slight further decrease (curve c). After the hybridization between the Ag NCs-DNA and MB that brought the CdS QDs and Ag NCs to close proximity, a sharp decrease about 61% in the photocurrent intensity could be observed as compared to the value of curve b (curve d). It

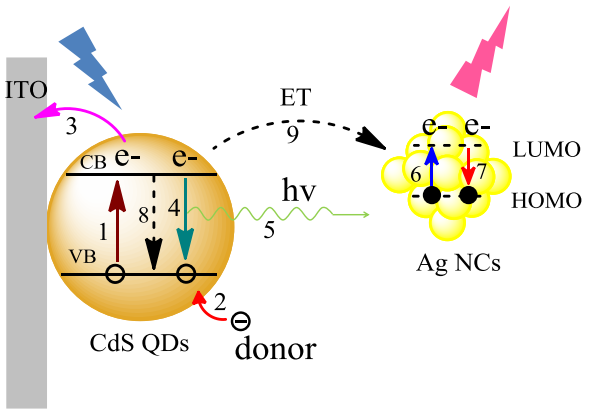

Scheme 2. Schematic illustration of the interparticle interaction between CdS QDs and Ag NCs in a PEC system. Process 1, photon absorption and electron transfer from the VB to the CB; Process 2, hole neutralization by electron donor; Process 3, electron ejection to the electrode for photocurrent generation; Process 4, radiative electron-hole recombination; Process 5, spontaneous emission originating from radiative decay; Process 6, electron transfer from the HOMO to the LUMO in Ag NCs; Process 7, radiative electron-hole recombination of Ag NCs; Process 8, nonradiative electron-hole recombination in CdS QDs; Process 9, energy transfer (ET) from CdS QDs to Ag NCs.

demonstrated that Ag NCs could cause an efficient quenching effect towards CdS QDs, also indicated the feasibility of the proposed protocol for DNA detection.

This phenomenon should be attributed to the interparticle interactions between the CdS QDs and the Ag NCs, and the explanation for current system was proposed as shown in Scheme 2. As illustrated, photoexcitation of the CdS QDs would result in the electron transfer from the valence band (VB) to the conduction band (CB), thus yielding the electron-hole pairs (Process 1). Once the exciton generated, they would be destined for the charge recombination or the spatial electron transfer and the concomitant hole neutralization (Process 2, 3). As shown in Fig. S3, upon 410 nm excitation, the CdS QDs has a broad emission range around 530 nm, which had a partial overlap with the excitation spectra of Ag NCs. On the other hand, composed of a few to a hundred atoms, the band structure of Ag NCs becomes discontinues and is broken down into discrete energy levels. However, Ag NCs can still interact with light via electronic transitions between energy levels, resulting in intense light absorption and emission. And it has been well-recognized that Ag NCs with distinct HOMO-LUMO gap is able to act like a semiconductor with small bandgap (Díez et al., 2011). So, in current system, the radiative decay (Process 4) in CdS QDs would result in the luminescence (Process 5) upon the nearby Ag NCs, rendering the excitation of the electrons from the HOMO to the LUMO of Ag NCs (Process 6) and the subsequent emission originated from the charge recombination (Process 7). More importantly, the presence of the Ag NCs would introduce an additional efficient nonradiative route (Process 8) for the excition relaxation in CdS QDs, and the energy transfer, which could be viewed as dipole-bipole interaction, would occur from the CdS QDs to the Ag NCs (Process 9) (Aldeek et al., 2013; Paramanik et al., 2016). Such process could greatly increase the excition recombination, thus decrease the spatial electron transfer and thereby significantly reduce the photocurrent of the system.

3.3. Analytical performance

Since the signal reduction in this PEC biosensor is directly related to the concentration of target DNA, an elegant PEC DNA biosensor could be realized via recording the signal changes. Specifically, more target DNA could unfold more MB, resulting in more binding of Ag NCs-DNA onto the electrode surface and hence

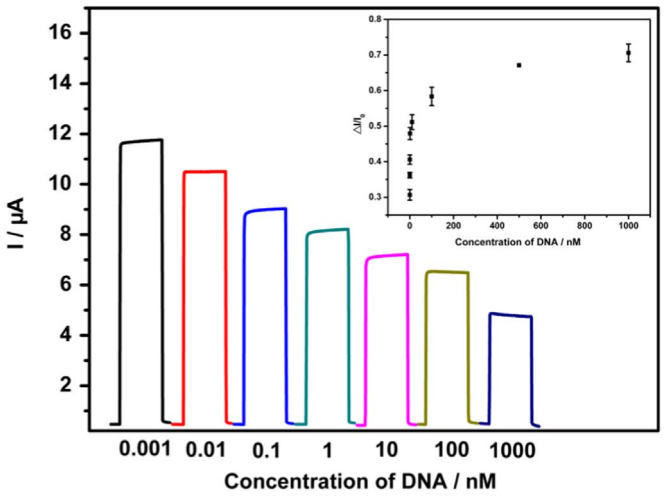

Fig. 3. Photocurrent responses of the modified electrode after different concentrations of target DNA and Ag NCs were anchored. Inset: effect of different concentrations of target DNA on the differential photocurrent responses ($\Delta I = I_0 - I$, I_0 and I are the photocurrents of target DNA and Ag NCs/MB/CdS/ITO electrode prior to and after hybridization respectively). The photocurrent measurement was carried out in 0.10 M PBS containing 0.10 M AA and the working potential was 0.0 V. The excitation wavelength was 410 nm.

more obvious signal attenuation. Fig. 3 presents the resulted photocurrent intensities corresponding to different concentrations of target DNA. As shown, the photocurrent reduction elevates with the increase of target DNA concentration, suggesting the target DNA-controlled unfolding of the MB and hence the enhanced Ag NCs loading for energy transfer inducement. Fig. 3 inset displays the quenching effects of the biosensor to different target DNA concentration. As shown in Fig. 4 the rate of photocurrent decrease was proportional to the target DNA concentration logarithmically with the linear range from 1.0 pM to 10 nM ($R^2 = 0.9862$) and detection limit was experimentally found to be of 0.3 pM. In addition, the performance of this protocol was further compared with other reported PEC DNA biosensors. As listed in Table 1, this biosensor possessed comparable or even better analytical performance than these reports.

In addition, the reproducibility of this PEC sensor was assessed by an interassay relative standard deviation (RSD). Five electrodes were used to assay 0.1 nM target and the RSD of 6.3% were

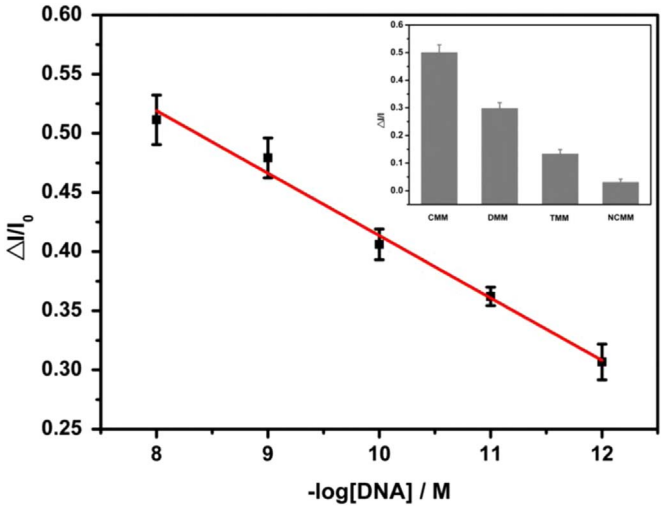

Fig. 4. The linear relationship between the relative photocurrent responses ($\Delta I/I_0$) and the target concentrations. Inset: selectivity of the proposed PEC bioanalysis by comparing the detection of 10 nM CMM, DMM, TMM and NCMM.

Table 1
Comparison of the analytical performance of some PEC DNA biosensors.

Detection method	Linear range (M)	LOD (M)	References
DNA conformational change	1.0×10^{-10}–8.0×10^{-9}	3.7×10^{-11}	Zhang et al. (2013d)
In situ generation of electron acceptor	1.0×10^{-12}–1.0×10^{-9}	8.0×10^{-13}	Zang et al. (2014)
Indicator-based technique	2.0×10^{-8}–4.0×10^{-7}	4.5×10^{-9}	Zhang et al. (2011)
Energy transfer-based technique	1.0×10^{-12}–1.0×10^{-8}	3.0×10^{-13}	This work

obtained, indicating the acceptable reproducibility. The selectivity of the Ag NCs based DNA PEC biosensor was investigated by detecting the photocurrent response to complementary target (CMM), double-base mismatched (DMM), three-base mismatched (TMM) and a non-complementary matched (NCMM) strands in the same concentration of 10 nM. As shown in Fig. 4 inset, the results demonstrated the acceptable specificity of the biosensor. Application of this biosensor for the real sample assay is under way.

4. Conclusion

In conclusion, we have introduced Ag NCs into a PEC nanosystem and exploited its interactions with CdS QDs for the first time, and it was found that the Ag NCs could quench the photoresponse of nearby CdS QDs obviously through an efficient interparticle energy transfer process. Based on this phenomenon, a simple protocol was designed for preliminary DNA detection. As a proof of concept, this work has demonstrated the enormous potential of Ag NCs in the dynamically developing field of PEC bioanalysis. When properly integrating with other engineered PEC nanosystems, the operating mechanism of our work can lead to many exciting opportunities for probing numerous other biorecognition or biocatalytic events.

Acknowledgements

We gratefully acknowledge the National Natural Science Foundation of China (Nos. 21327902, 21135003, 21273114 and 21305063), the Natural Science Funds of Jiangsu Province (BK20130553), the Fundamental Research Funds for the Central Universities (Grant No. NE2015003), and the “Six Talent Peaks Program” of Jiangsu Province (Grant No. 2013-XNY-010) for support. This work was also supported by a Project Funded by the Priority Academic Program Development of Jiangsu Higher Education Institutions.

Appendix A. Supplementary material

Supplementary data associated with this article can be found in the online version at http://dx.doi.org/10.1016/j.bios.2016.06.018.

References

Aldeek, F., Ji, X., Mattoussi, H., 2013. J. Phys. Chem. C 117, 15429–15437.
Díez, I., Ras, R.H.A., 2011. Nanoscale 3, 1963–1970.
Dong, H., Jin, S., Ju, H., Hao, K., Xu, L.P., Lu, H., Zhang, X., 2012. Anal. Chem. 84, 8670–8674.
Fang, Y.M., Song, J., Li, J., Wang, Y.W., Yang, H.H., Sun, J.J., Chen, G.N., 2011. Chem. Commun. 47, 2369–2371.
Gill, R., Zayats, M., Willner, I., 2008. Angew. Chem. Int. Ed. 47, 7602–7625.
Gong, L., Kuai, H., Ren, S., Zhao, X.H., Huan, S.Y., Zhang, X.B., Tan, W., 2015. Chem. Commun. 51, 12095–12098.
Guével, X.L., Spies, C., Daum, N., Jung, G., Schneider, M., 2012. Nano Res. 5, 379–387.
Han, B.Y., Wang, E.K., 2012. Anal. Bioanal. Chem. 402, 129–138.
Li, H.B., Qiao, Y.F., Li, J., Fang, H.L., Fan, D.H., Wang, W., 2016. Biosens. Bioelectron. 77, 378–384.
Li, L.L., Liu, H.Y., Shen, Y.Y., Zhang, J.R., Zhu, J.J., 2011. Anal. Chem. 83, 661–665.
Link, S., Beeby, A., FitzGerald, S., El-Sayed, M.A., Gregory Schaaff, T., Whetten, R.L., 2002. J. Phys. Chem. B 106, 3410–3415.
Liu, X.R., Hu, R.X., Gao, Z.D., Shao, N., 2015. Langmuir 31, 5859–5867.
Long, Y.T., Kong, C., Li, D.W., Li, Y., Chowdhury, S., Tian, H., 2011. Small 12, 1624–1628.
Ma, Z.Y., Ruan, Y.F., Xu, F., Zhao, W.W., Xu, J.J., Chen, H.Y., 2016. Anal. Chem. 88, 3864–3871.
Ma, Z.Y., Ruan, Y.F., Zhang, N., Zhao, W.W., Xu, J.J., Chen, H.Y., 2015. Chem. Commun. 51, 8381–8384.
Paramanik, B., Kundu, S., De, G., Patra, A., 2016. J. Mater. Chem. C 4, 486–496.
Richards, C.I., Choi, S., Hsiang, J.C., Antoku, Y., Vosch, T., Bongilrno, A., Tzeng, Y.L., Dickson, R.M., 2008. J. Am. Chem. Soc. 130, 5038–5039.
Ritchie, C.M., Johnsen, K.R., Kiser, J.R., Antoku, Y., Dickson, R.M., Petty, J.T., 2007. J. Phys. Chem. C 111, 175–181.
Shang, L., Dong, S.J., Ulrich Nienhaus, G., 2011. Nano Today 6, 401–418.
Shu, J., Qiu, Z.L., Zhou, Q., Lin, Y.X., Lu, M.H., Tang, D.P., 2016. Anal. Chem. 88, 2958–2966.
Sun, G.Q., Zhang, Y., Kong, Q.K., Zheng, X.X., Yu, J.H., Song, X.R., 2015. Biosens. Bioelectron. 66, 567–571.
Tang, J., Li, J. Da, Wang, P.M., Zheng, G.F, Y.C., 2015. Chem. Eur. J. 21, 11288–11299.
Wang, G.L., Liu, K.L., Shu, J.X., Gu, T.T., Wu, X.M., Dong, Y.M., Li, Z.J., 2015. Biosens. Bioelectron. 69, 106–112.
Wang, G.L., Yu, P.P., Xu, J.J., Chen, H.Y., 2009. J. Phys. Chem. C 113, 11142–11148.
Wang, M., Yin, H.S., Shen, N.N., Xu, Z.N., Sun, B., Ai, S.Y., 2014a. Biosens. Bioelectron. 53, 232–237.
Wang, Y., Dai, C., Yan, X.P., 2014b. Chem. Commun. 50, 14341–14344.
Xiao, Y., Shu, F., Wong, K.Y., Liu, Z.H., 2013. Anal. Chem. 85, 8493–8497.
Yan, Y.T., Liu, Q., Du, X.J., Qian, J., Mao, H.P., Wang, K., 2015. Anal. Chim. Acta 853, 258–264.
Yeh, H.C., Sharma, J., Han, J.J., Martinez, J.S., Werner, J.H., 2010. Nano Lett. 10, 3106–3110.
Zang, Y., Lei, J.P., Zhang, L., Ju, H.X., 2014. Anal. Chem. 86, 12362–12368.
Zeng, X.X., Ma, S.S., Bao, J.C., Tu, W.W., Dai, Z.H., 2013. Anal. Chem. 85, 11720–11724.
Zhang, M., Guo, S.M., Li, Y.R., Zuo, P., Ye, B.C., 2012a. Chem. Commun. 48, 5488–5490.
Zhang, X.R., Xu, Y.P., Yang, Y.Q., Jin, X., Ye, S.J., Zhang, S.S., Jiang, L.L., 2012b. Chem. Eur. J. 18, 16411–16418.
Zhang, L.B., Zhu, J.B., Guo, S.J., Li, T., Li, J., Wang, E.K., 2013a. J. Am. Chem. Soc. 135, 2403–2406.
Zhang, L.B., Zhu, J., Zhou, Z.X., Guo, S.J., Li, J., Dong, S.J., Wang, E.K., 2013b. Chem. Sci. 4, 4004–4010.
Zhang, X.R., Guo, Y.S., Liua, M.S., Zhang, S.S., 2013c. RSC Adv. 3, 2846–2857.
Zhang, X.R., Xu, Y.P., Zhao, Y.Q., Song, W.L., 2013d. Biosens. Bioelectron. 39, 338–341.
Zhang, X.R., Zhao, Y.Q., Zhou, H.R., Qu, B., 2011. Biosens. Bioelectron. 26, 2737–2741.
Zhao, W.W., Wang, J., Xu, J.J., Chen, H.Y., 2011. Chem. Commun. 47, 10990–10992.
Zhao, W.W., Xu, J.J., Chen, H.Y., 2014. Chem. Rev. 114, 7421–7441.
Zhao, W.W., Yu, P.P., Shan, Y., Wang, J., Xu, J.J., Chen, H.Y., 2012. Anal. Chem. 84, 5892–5897.
Zheng, X.Y., Yao, T.M., Zhu, Y., Shi, S., 2015. Biosens. Bioelectron. 66, 103–108.
Zhuang, J.Y., Lai, W.Q., Xu, M.D., Zhou, Q., Tang, D.P., 2015. ACS Appl. Mater. Interfaces 7, 8330–8338.